

Upper Bounds on the Superfluid Stiffness of Disordered Systems

Arun Paramekanti*, Nandini Trivedi †, and Mohit Randeria ‡
Theoretical Physics Group, Tata Institute of Fundamental Research, Mumbai 400005, India

We derive several upper bounds for the superfluid stiffness D_s for Bose and Fermi systems in terms of expectation values of local operators using linear response theory and variational methods. These give insight into the non-trivial dependence of D_s on parameters such as disorder and interaction in systems with broken continuous translational invariance. Our best variational bound for disordered systems is obtained by allowing the phase twist applied at the boundary to be distributed inhomogeneously within the system. Path integral quantum Monte Carlo simulations are used to quantitatively compare the bounds and D_s for disordered interacting Bose systems.

I. Introduction:

The superfluid density n_s , or the closely related stiffness D_s (defined below), characterizes the phase rigidity of a superconductor or a superfluid. Experimentally n_s is more easily measured than the order parameter since external probes, such as magnetic fields or rotation, can couple to the relevant correlation function. Further, even from a theoretical point of view, n_s is arguably the more fundamental characterization: e.g., in two dimensional systems n_s can be non-zero even though the order parameter vanishes at finite temperatures.

In translationally invariant (one component) superfluid systems, it can be shown on general grounds that at $T = 0$, $n_s = n$, the total density: all of the fluid participates in superflow [1]. This follows from translational invariance and the absence of low lying excitations that can couple to a transverse probe. However, as soon as one destroys continuous translational invariance, either by the presence of a lattice or impurities, n_s is no longer constrained to be the total density n , and becomes smaller as we shall describe below. The dependence of n_s at $T = 0$ on disorder is of considerable interest since with increasing disorder one could suppress the superfluid density and eventually drive the system into a non-superfluid, possibly insulating state [2,3].

In this paper we will derive exact upper bounds on n_s (or D_s) which help understand how the superfluid density varies with interaction and disorder in both Fermi and Bose systems. An outline of the paper and a summary of our main results is as follows. Section II introduces the notation and definitions used in the rest of the paper. In Section III we discuss bounds for D_s obtained from linear response theory, emphasizing the effect of breaking continuous translational invariance. Two simple upper bounds, eqn. (10) and eqn. (12), are derived and compared with results of path integral quantum Monte Carlo (QMC) simulations for non-disordered lattice boson problems.

In Section IV we derive variational upper bounds on D_s for a system with disorder by constructing a trial wave function for a system with twisted boundary conditions given the exact ground state for the untwisted case. We obtain two bounds: one, D_s^o given in eqn. (21), which is the lattice analog of a result derived earlier by Leggett [4] for continuum systems, and an improved variational bound D_s^* given in eqn. (18). The calculation of D_s^* is shown to be equivalent to calculating the conductance of a resistor network problem as explained in the discussion following eqn. (18). We also briefly discuss the generalization of these results to finite temperature.

The physical idea underlying the bounds D_s^o and D_s^* is the following. In a homogeneous system the applied twist at the boundaries is distributed uniformly across the entire system. However, in an inhomogeneous system the twist is accommodated preferentially in those regions of space where it costs the least energy, leading to a lower stiffness. Our results can be summarized by the following set of inequalities

$$D_s \leq D_s^* \leq D_s^o \leq \pi \langle K_1 \rangle \leq 2t\pi\bar{n} \quad (1)$$

*arun@theory.tifr.res.in

†ntrivedi@theory.tifr.res.in

‡randeria@theory.tifr.res.in

where D_s is the exact superfluid stiffness, D_s^o and D_s^* are the bounds mentioned above, $\langle K_1 \rangle$ is (the absolute value of) the mean kinetic energy (KE) on a bond, t is the hopping strength in the lattice model and \bar{n} is the filling or the average particle density.

In Section V we illustrate the quantitative usefulness of our results by discussing various examples and comparing the bounds with D_s obtained from QMC calculations on disordered Bose systems. (The details of the QMC are given in the Appendix.) The bounds are found to capture the non-trivial parameter dependence of D_s , including its nonmonotonic variation in some cases. However, these bounds, which are based on local correlation functions, are not in general sensitive to the superfluid-insulator transition. In Section VI, we make several remarks about our results. Amongst other things we briefly discuss charge vs superfluid stiffness, describe a model for which D_s^* captures a percolation transition that is missed by the other bounds, and obtain bounds on T_c for 2D systems. We summarize our results in Section VII.

II Definitions and Notation

We consider interacting Bose or Fermi systems with a generic Hamiltonian

$$\hat{H} = - \sum_{\mathbf{r}, \alpha=1 \dots d} t_\alpha(\mathbf{r}) [c^\dagger(\mathbf{r})c(\mathbf{r} + \hat{\alpha}) + h.c.] + \hat{V}. \quad (2)$$

We work on a hypercubic lattice in d dimensions with lattice spacing $a = 1$, \mathbf{r} runs over all $N = L^d$ lattice sites and $\hat{\alpha}$ denotes the unit vector along the α^{th} direction. c and c^\dagger are annihilation and creation operators; for Fermi systems we may also need spin labels which are omitted for simplicity. \hat{V} includes all possible interactions between the particles as well as the possibly random (one-body) potential and is an operator which is diagonal in the number basis. Finally, $t_\alpha(\mathbf{r})$ is the hopping amplitude between nearest neighbour sites \mathbf{r} and $\mathbf{r} + \hat{\alpha}$. This may again be a random function but is restricted to be positive. (Note that we do *not* consider frustration introduced by having both positive and negative hopping amplitudes.)

The kinetic energy operator on the link $(\mathbf{r}, \mathbf{r} + \hat{\alpha})$ is defined as

$$K_\alpha(\mathbf{r}) = t_\alpha(\mathbf{r}) [c^\dagger(\mathbf{r})c(\mathbf{r} + \hat{\alpha}) + h.c.]. \quad (3)$$

For later convenience, this definition differs from the standard one by a negative sign. The paramagnetic current along $\hat{\alpha}$ at point \mathbf{r} is given by

$$j_\alpha(\mathbf{r}) = -it_\alpha(\mathbf{r}) [c^\dagger(\mathbf{r})c(\mathbf{r} + \hat{\alpha}) - h.c.]. \quad (4)$$

The (paramagnetic) current-current correlation function for an $N = L^d$ site system at zero temperature and zero frequency is given by

$$\chi_1(\mathbf{q}, \omega = 0) = \frac{2}{N} \sum_{n \neq 0} \frac{\overline{|\langle \psi_n | j_1(\mathbf{q}) | \psi_0 \rangle|^2}}{\omega_n - \omega_0} \quad (5)$$

where $|\psi_n\rangle$ is the n^{th} eigenstate of the system with energy ω_n ($n = 0$ denotes the ground state) and \mathbf{q} is the momentum. The overbar denotes an average over the quenched disorder. (This is a shorthand notation for first evaluating the correlation function in real space, then disorder averaging and finally Fourier transforming to momentum space.) Now, within the Kubo formalism, we can define the superfluid stiffness D_s in terms of the transverse current-current correlation [5,6]:

$$\frac{D_s}{\pi} = \langle \psi_0 | K_1 | \psi_0 \rangle - \chi_1(q_1 = 0, \mathbf{q}_\perp \rightarrow 0, \omega = 0) \quad (6)$$

where $\mathbf{q}_\perp = \{q_2, \dots, q_d\}$ is the set of momentum coordinates orthogonal to the $\hat{1}$ direction. The first term $\langle K_1 \rangle \equiv L^{-d} \sum_{\mathbf{r}} \langle \psi_0 | K_1(\mathbf{r}) | \psi_0 \rangle$ comes from the diamagnetic part of the response [7].

An equivalent definition of the superfluid stiffness is arrived at by using twisted boundary conditions (b.c.) on the ground state wave function [8,9]. This can be imposed in the standard way by considering the system as a “ring” in the $\hat{1}$ direction, threaded by a flux Φ . (Note that $\Phi = 0$ corresponds to periodic b.c.’s). In the site-occupation basis, moving one particle around the ring, keeping the others

fixed, amounts to changing the configuration from $\{n\} \equiv \{n(\mathbf{r}_1), \dots, n(\mathbf{r}_m), \dots, n(\mathbf{r}_N)\}$ with $n(\mathbf{r}_m) \geq 1$, to $\{n'\} \equiv \{n(\mathbf{r}_1), \dots, n(\mathbf{r}_m) - 1, \dots, n(\mathbf{r}_N); n(\mathbf{r}_m + \hat{\mathbf{L}}) = 1\}$. The twisted b.c. is then given by

$$\langle \{n'\} | \psi_\Phi \rangle = e^{i\Phi} \langle \{n\} | \psi_\Phi \rangle. \quad (7)$$

The increase in ground state energy $E(\Phi) = \langle \psi_\Phi | \hat{H} | \psi_\Phi \rangle$ for a small applied twist

$$E(\Phi) - E(0) = \frac{1}{2} \frac{D_s}{\pi} L^d \left(\frac{\Phi}{L} \right)^2 + \dots \quad (8)$$

defines the superfluid stiffness D_s . This is related to the superfluid density n_s and the helicity modulus Υ [9] via

$$\frac{D_s}{\pi} = L^{2-d} \lim_{\Phi \rightarrow 0} \frac{\partial^2 E(\Phi)}{\partial \Phi^2} = 2t n_s = \Upsilon. \quad (9)$$

Note that for a disordered system, the twist definition of D_s is valid for any given disorder realization, and thus disorder averaging can be done at the end of the calculation.

The generalization of the above definitions of D_s to finite temperatures is straightforward. In the Kubo formula (5) and (6), the ground state expectation value has to be replaced by a thermal average, and correspondingly in the twisted b.c. formulation (9) the energy has to be replaced by the free energy.

III Bounds from Linear Response Theory

From (5) we see that $\chi_1(\mathbf{q}, \omega = 0)$ is non-negative. It then follows from (6) that

$$D_s/\pi \leq \langle K_1 \rangle. \quad (10)$$

At finite temperatures the right hand side should be viewed as thermal expectation value.

This bound can be further simplified for the case of uniform hopping $t_\alpha(\mathbf{r}) \equiv t$. Using the Cauchy-Schwarz inequality and the fact that the geometric mean is less than the arithmetic mean we find

$$\langle K_1(\mathbf{r}) \rangle \equiv t \langle (c^\dagger(\mathbf{r})c(\mathbf{r} + \hat{\mathbf{1}}) + h.c.) \rangle \leq 2t \sqrt{n(\mathbf{r})n(\mathbf{r} + \hat{\mathbf{1}})} \leq t(n(\mathbf{r}) + n(\mathbf{r} + \hat{\mathbf{1}})), \quad (11)$$

where $n(\mathbf{r}) \equiv \langle c^\dagger(\mathbf{r})c(\mathbf{r}) \rangle$. Further $\langle K_1 \rangle \leq t L^{-d} \sum_{\mathbf{r}} (n(\mathbf{r}) + n(\mathbf{r} + \hat{\mathbf{1}})) = 2t\bar{n}$ and using (9) we get

$$n_s \leq \langle K_1 \rangle / 2t \leq \bar{n}. \quad (12)$$

Thus, the superfluid density for an interacting lattice or disordered system can be, and in general is, less than the average particle density. The aim of this paper is to understand how this happens and (in the following Sections) to derive bounds that improve upon the ones above. In the present section we focus on the non-disordered problem; we turn to the the disordered problem in later sections.

Let us begin by emphasizing the importance of broken continuous translational invariance for $n_s(T = 0)$. For a translationally invariant system, the diamagnetic piece (the analog of $\langle K_1 \rangle$ in (6)) is given by \bar{n} . Furthermore the $\mathbf{q} = 0$ current operator is the total momentum which commutes with the Hamiltonian, leading to a vanishing numerator in (5). Thus for a continuum superfluid χ_1 vanishes and $n_s(T = 0) = \bar{n}$ [1] since there are no low lying excitations which can couple to a transverse probe. (The only low lying excitations present are longitudinal phonons, and even these may be gapped for a charged system). However in the presence of a lattice or impurities, the total ($\mathbf{q} = 0$) current operator does *not* commute with the Hamiltonian in general, thus χ_1 is non-zero, and (10) is in fact a *strict* upper bound on the stiffness.

It is important to note that approximate treatments can miss out on the paramagnetic current correlation piece and give just the diamagnetic part *even* on the lattice. For example, the BCS mean field theory for superconductors reduces the problem to one of non-interacting particles (Bogoliubov quasiparticles) with a gapped spectrum and a current operator which commutes with the reduced BCS Hamiltonian (even on a lattice). Thus, estimating the reduction of the superfluid stiffness from its diamagnetic value at $T = 0$ requires including fluctuations beyond mean field theory [10].

We next discuss interacting (non-disordered) Bose systems on a lattice to illustrate the usefulness of the bound (10). We consider the 2D boson Hubbard model with Hamiltonian

$$\hat{H}_{\text{bose}} = -t \sum_{\mathbf{r}, \alpha=1 \dots d} [c^\dagger(\mathbf{r})c(\mathbf{r} + \hat{\alpha}) + h.c.] + \frac{U}{2} \sum_{\mathbf{r}} \hat{n}(\mathbf{r}) [\hat{n}(\mathbf{r}) - 1] \quad (13)$$

where $\hat{n}(\mathbf{r}) = c^\dagger(\mathbf{r})c(\mathbf{r})$. By comparing the bound with exact results from QMC simulations on finite two-dimensional lattices, we gain insight into how the superfluid stiffness for lattice systems depends on the interaction, unlike in the continuum case. The calculation of D_s from QMC is described in the Appendix. Here we summarize relevant numerical details. The QMC simulations have been done on lattices of size $N = 6 \times 6$ at commensurate and incommensurate fillings with filling fractions $\bar{n} = 1$ and $\bar{n} = 1/2$ respectively. The inverse temperature $\beta t = 4$ is discretised into $N_\tau = 32$ steps which implies that $\delta\tau \equiv \beta/N_\tau = 1/8$ is the elementary time step on which the Trotter approximation is done. We averaged over 10^8 MC sweeps through the space-time lattice with 10^6 equilibration sweeps during which we did not collect data. The very large number of sweeps was necessary to get small enough error bars for the superfluid stiffness D_s in order to distinguish the QMC results from the bounds, especially for large interaction and (or) disorder which is the region of parameter space explored in both this as well as later sections. The calculations for each data point took approximately 36 hours on a 100 MHz pentium.

In all figures, here and below, we will plot the superfluid stiffness normalized such that it is unity for the noninteracting clean (no disorder) problem at $T = 0$, independent of the filling factor. We normalize the bounds also by the same factor. Thus, at $T = 0$, what we plot for the stiffness is really n_s/\bar{n} as can be seen from the definitions above since $n_s = \bar{n}$ for the clean noninteracting problem at zero temperature.

First consider the case of incommensurate (non-integral) filling where the system is expected to be superfluid for all values of the interaction strength $0 \leq U \leq \infty$. We see from Fig. 1 that the superfluid stiffness D_s , though non-zero for all U , decreases monotonically with the repulsion U . The bound $\pi\langle K_1 \rangle$ derived in eqn.(10) tracks the behavior of D_s fairly well even at large U . The error bars on the bounds are much smaller than those on D_s and are hence not indicated in Fig. 1 or any of the subsequent figures.

Next, consider a commensurate filling of one boson per site (on average). With increasing U we expect a Mott transition [2] from a superfluid into a Mott insulator at a critical value $U = U_c$. Our aim here is not to locate and characterize this transition very precisely (which would require a finite size scaling analysis of the QMC data as in Ref. [11]). In Fig. 2, we compare the KE bound with D_s obtained from QMC on the finite lattice. Even though the bound captures the overall decreasing trend of D_s , it falls off as t^2/U for large U (as expected from perturbation theory) rather than vanishing like D_s for roughly $U \geq 20$. Being a purely local quantity the KE bound misses the transition. This brings out the importance of the excitations which contribute to χ_1 and reduce the stiffness from its diamagnetic value eventually driving D_s to zero at the transition.

It hardly needs to be emphasized that any non-zero upper bound on D_s such as (10), though valid, will not be useful for systems which are in fact *non*-superfluid (metallic or insulating). In such cases the paramagnetic piece χ_1 ignored in the bound (10) must exactly cancel $\langle K_1 \rangle$, leading to $D_s = 0$. The most trivial example is the non-interacting fermi gas: the total current operator commutes with the Hamiltonian even on a lattice, leading to a vanishing numerator in the paramagnetic term in (5), but the low lying particle-hole excitations contribute in such a way that there is complete cancellation between the diamagnetic and paramagnetic terms in (6). More non-trivial examples are the Mott phase of the boson Hubbard model discussed above, as well as the large U (fermion) Hubbard model at half-filling, which is also a Mott insulator. In both cases, the total current operator no longer commutes with the Hamiltonian and the high energy states (excitations across the charge gap) contribute to χ_1 leading once again to a complete cancellation in (6).

IV. Variational Bounds

We now turn to the task of improving upon the bounds of the previous Section, especially for disordered systems described by the Hamiltonian in eqn.(2) for an interacting Bose or Fermi system in the presence of a site-dependent disorder potential. To this end we use a variational method first suggested by Leggett [4]; see also [12]. Although these authors worked in a first quantized representation, we find it more convenient to work in the occupation number basis. Let us assume that the *exact* (normalized) ground

state $|\psi_0\rangle$ of the Hamiltonian (2) with periodic boundary conditions (b.c.) in all directions is known. We make an ansatz $|\psi_\Phi\rangle$ for the ground state of (2) subject to the twisted b.c. (7) along the $\hat{1}$ direction, with periodic boundary conditions in the other $(d-1)$ directions. Let:

$$|\psi_\Phi\rangle = \exp \left[i \sum_{\mathbf{r}} \theta(\mathbf{r}) \hat{n}(\mathbf{r}) \right] |\psi_0\rangle \quad (14)$$

where \mathbf{r} runs over all lattice sites and $\theta(\mathbf{r})$ are the variational parameters at our disposal. The twisted b.c. (7) imposes the constraint

$$\theta(r_1 = L+1, \mathbf{r}_\perp) - \theta(r_1 = 1, \mathbf{r}_\perp) = \Phi. \quad (15)$$

where r_1 is the coordinate in the $\hat{1}$ direction along which the twist is applied and $\mathbf{r}_\perp \equiv r_2, \dots, r_d$ refers to the set of coordinates transverse to this direction. The variational estimate for the difference in energy between the twisted and the untwisted boundary condition cases is then (for small twist);

$$\begin{aligned} \Delta E_{\text{trial}}[\Phi] &= \langle \psi_\Phi | H | \psi_\Phi \rangle - \langle \psi_0 | H | \psi_0 \rangle \\ &= \frac{1}{2} \sum_{\mathbf{r}, \alpha=1 \dots d} (\theta(\mathbf{r}) - \theta(\mathbf{r} + \hat{\alpha}))^2 \langle K_\alpha(\mathbf{r}) \rangle \end{aligned} \quad (16)$$

where $\langle K_\alpha(\mathbf{r}) \rangle = \langle \psi_0 | K_\alpha(\mathbf{r}) | \psi_0 \rangle$. (In this expression the term linear in $[\theta(\mathbf{r}) - \theta(\mathbf{r} + \hat{\alpha})]$ vanishes, since we assume that the ground state $|\psi_0\rangle$ does not break time-reversal symmetry and is thus real and carries no current on any link.) Minimizing ΔE_{trial} with respect to the parameters $\theta(\mathbf{r})$ (for those \mathbf{r} *not* on the boundary on which the twist is applied) we obtain the following set of equations:

$$\sum_{\alpha=1 \dots d} \{ \langle K_\alpha(\mathbf{r}) \rangle [\theta(\mathbf{r}) - \theta(\mathbf{r} + \hat{\alpha})] + \langle K_{-\alpha}(\mathbf{r}) \rangle [\theta(\mathbf{r}) - \theta(\mathbf{r} - \hat{\alpha})] \} = 0 \quad (17)$$

where we have defined $K_{-\alpha}(\mathbf{r}) = t_{-\alpha}(\mathbf{r}) [c^\dagger(\mathbf{r}) c(\mathbf{r} - \hat{\alpha}) + h.c.]$ in parallel with (3).

There are in all $L^d - L^{d-1}$ equations implied by eqn.(17) and L^{d-1} equations implied by the constraint eqn.(15) thus giving us a total of L^d equations which allows us to solve for the phase $\theta^*(\mathbf{r})$ at each point of the lattice. The solution $\{\theta^*(\mathbf{r})\}$ of equations (17) and (15) defines the optimal choice of the local phases in $|\psi_\Phi\rangle$ in response to the applied twist. This in turn determines D_s^* via the relation

$$\frac{1}{2} \frac{D_s^*}{\pi} L^{d-2} (\Phi)^2 = \Delta E_{\text{trial}}^* = \frac{1}{2} \sum_{\mathbf{r}, \alpha=1 \dots d} (\theta^*(\mathbf{r}) - \theta^*(\mathbf{r} + \hat{\alpha}))^2 \langle K_\alpha(\mathbf{r}) \rangle. \quad (18)$$

It follows from the variational principle that $\Delta E_{\text{trial}}^*[\Phi] \geq \Delta E[\Phi]$ and thus $D_s^* \geq D_s$ from eqn.(18) above.

It is not possible to start from the set of equations (17) and (15), and arrive at an analytic closed form solution for the bound D_s^* in general in $d > 1$. (Later we will discuss the $d = 1$ case and also a simplified form which admits an analytic solution in arbitrary dimension). It is however possible to calculate D_s^* numerically solving the linear equations (15) and (17). For this, we first map the problem of obtaining D_s^* on to a particular *random resistor network* problem which gives us some intuition for the results. The lattice points \mathbf{r} of the above system form the nodes of the network, $\theta(\mathbf{r})$ is the voltage at node \mathbf{r} , and $\langle K_{\pm\alpha}(\mathbf{r}) \rangle$ is the conductance of the link $(\mathbf{r}, \mathbf{r} \pm \hat{\alpha})$. The equations (17) represent (Kirchoff) current conservation at each node \mathbf{r} , and the constraint (15) is a constant voltage Φ maintained across this *resistor network*. The quantity to be minimised in eqn. (16) is the (Joule) heat dissipation in the network. Thus $L^{d-2} D_s^* / \pi$, defined by (18), is the *conductance* of an equivalent resistor which dissipates the same amount of heat as the network for the same voltage difference across its ends.

It is instructive to write down the solution to the above equations in $d = 1$ where a closed form result can be obtained. We find

$$\theta^*(x+1) - \theta^*(x) = \frac{\Phi}{\langle K_1(x) \rangle} \frac{1}{\sum_{x=1 \dots L} \langle K_1(x) \rangle^{-1}}, \quad (19)$$

from which we get $D_s^* = L\pi K_{\text{tot}}$ with

$$\frac{1}{K_{\text{tot}}} = \sum_{x=1 \dots L} \frac{1}{\langle K_1(x) \rangle}. \quad (20)$$

It is easy to see that $1/K_{\text{tot}}$ is simply the total resistance of the 1-d network obtained by adding the resistances of the links in series. In order to help visualise this result, we show exact diagonalization results for a system of bosons on a finite one dimensional lattice in Fig. 3. The Hamiltonian used is $H_{\text{bose}} + \sum_{\mathbf{r}} V(\mathbf{r}) \hat{n}(\mathbf{r})$ where H_{bose} is defined in eqn.(13). The parameter values chosen are given in the figure. We plot the way the imposed phase twist at the boundary is accommodated along the chain, and find that a large phase twist occurs across bonds where the local kinetic energy is small as expected from eqn. (19).

The $d = 1$ result suggests a simple generalization to arbitrary d . If we assume that $\theta(\mathbf{r})$ depends only on r_1 , the coordinate along the applied twist direction, and is independent of the transverse coordinates $\mathbf{r}_\perp \equiv \{r_2, \dots, r_d\}$ then (following the steps in the derivation of (18)) we get an explicit analytic expression for the bound D_s^o as

$$\frac{D_s}{\pi} \leq \frac{D_s^o}{\pi} = L^{2-d} \frac{1}{\sum_{r_1} [\sum_{\mathbf{r}_\perp} \langle K_1(r_1, \mathbf{r}_\perp) \rangle]^{-1}} \quad (21)$$

where $\langle K_1(r_1, \mathbf{r}_\perp) \rangle \equiv \langle K_1(\mathbf{r}) \rangle$. We note that D_s^o is the lattice analog of the continuum result obtained by Leggett [4] and Chester [12]; in the continuum $K_1(\mathbf{r})$ gets replaced by the density $n(\mathbf{r})$. The two bounds D_s^* and D_s^o coincide in one dimension as seen from (20) and (21). The two bounds also coincide for the non-disordered problem in any d ; the (discrete) translational invariance ensures that the bound is just the mean kinetic energy on the links in the direction of the applied twist. However, in general, for $d > 1$, $D_s^* < D_s^o$ and is a better bound because it has more variational parameters [13].

We have thus derived all the inequalities in (1), except for the third: $D_s^o \leq \pi \langle K_1 \rangle$. The first two inequalities were derived above and the last one in (1), valid only for systems with uniform hopping, was derived in (12). To complete our task, we use the inequality $M^{-1} \sum_i a_i \geq [M^{-1} \sum_i a_i^{-1}]^{-1}$ for positive numbers a_i , $i = 1, \dots, M$, in (21). This yields

$$\frac{D_s^o}{\pi} \leq L^{2-d} \frac{1}{L^2} \sum_{r_1} \frac{1}{(\sum_{\mathbf{r}_\perp} \langle K_1(r_1, \mathbf{r}_\perp) \rangle)^{-1}} = \langle K_1 \rangle. \quad (22)$$

Generalization to Finite Temperatures

The above bounds can be easily generalised to finite temperatures using a trial (variational) density matrix as sketched below. This can be easily shown to lead to the same equations as the zero temperature case with the only difference being that we get thermal expectation values instead of ground state expectation values for the local kinetic energies. This allows us to compare the bounds with the QMC results for D_s in the next section. The local kinetic energies needed for calculating the bounds are also obtained using QMC as described in the Appendix.

Let $\hat{\rho}_0 = \sum_m e^{-\beta E_m} |m\rangle \langle m|$ be the density matrix for the untwisted case, where $|m\rangle$ denotes the eigenstate of energy E_m for the system with untwisted boundary conditions. Consider a trial density matrix for the twisted case of the form

$$\hat{\rho}(\Phi) = \exp[i \sum_{\mathbf{r}} \hat{n}(\mathbf{r}) \theta(\mathbf{r})] \hat{\rho}_0 \exp[-i \sum_{\mathbf{r}} \hat{n}(\mathbf{r}) \theta(\mathbf{r})]. \quad (23)$$

with boundary conditions as in eqn(15). The trial free energy is given by

$$F(\Phi) \leq F_{\text{trial}}(\Phi) = \text{Tr}[\hat{\rho}(\Phi) \hat{H}] + \beta^{-1} \text{Tr}[\hat{\rho}(\Phi) \ln \hat{\rho}(\Phi)] \quad (24)$$

and we need to minimize $F_{\text{trial}}(\Phi)$ as before. Using the unitary nature of the transformation in eqn.(23) and the cyclic property of the trace, it is straightforward to show that the entropy term $\beta^{-1} \text{Tr}[\hat{\rho}(\Phi) \ln \hat{\rho}(\Phi)]$ remains unchanged even when the twist is put in. The energy term $\text{Tr}(\hat{\rho}(\Phi) \hat{H})$ leads to an expression identical to that obtained at $T = 0$ with thermal expectation values instead.

V. Comparison with Quantum Monte Carlo Results:

In this Section we illustrate the usefulness of the bounds by comparing them with the stiffness D_s obtained from QMC [14,15] for interacting Bose systems described by the Hamiltonian in eqn.(2) with $t_\alpha(\mathbf{r}) = t$ and

$$\hat{V} = \frac{U}{2} \sum_{\mathbf{r}} \hat{n}(\mathbf{r})(\hat{n}(\mathbf{r}) - 1) + \sum_{\mathbf{r}} V(\mathbf{r})\hat{n}(\mathbf{r}) \quad (25)$$

We work in two dimensions and choose the site dependent (disorder) potential $V(\mathbf{r})$ as given below for various cases.

We first consider a particular case of broken (discrete) translational invariance to illustrate the difference between the various bounds in (1). We choose a certain set of sites on the lattice where $V(\mathbf{r}) = V > 0$ (marked in the inset to Fig. 4) while fixing the potential at other sites to be zero. We then study the effect of varying V on the superfluid stiffness D_s and compare it with the various bounds, all computed for a twist applied along the x -direction. The results are shown in Fig. 4: as V is increased, the mean KE bound and D_s^o are both considerably larger than the true stiffness while the bound D_s^* tracks the true stiffness extremely well. For instance at large V , as seen from Fig. 4, $\langle K_1 \rangle \sim 0.8$, $D_s^o/2\pi\bar{n}t \sim 0.5$, while $D_s^*/2\pi\bar{n}t$ and $D_s/2\pi\bar{n}t$ are both ~ 0.05 and thus D_s^* is about an order of magnitude better than the other bounds. We do not know if the excellent agreement between D_s^* and D_s would persist in the thermodynamic limit, nevertheless it is clear that D_s^* does considerably better than the other bounds.

We next consider the disordered Boson Hubbard model, which is defined by (25), with $V(\mathbf{r})$ at each \mathbf{r} an independent random variable uniformly distributed in the interval $[-V_{\text{dis}}, V_{\text{dis}}]$. We study the case of incommensurate filling, i.e., non-integral average site occupancy. As mentioned earlier, the bounds are valid for any given disorder realization. We therefore choose to consider a particular realization of the random potential in Figs. 5 and 6 in order to illustrate the bounds.

In Fig. 5 we keep the disorder strength V_{dis} fixed, and look at the interaction U -dependence of the superfluid stiffness and the bounds. For small U , we see that D_s is small, since at $U = 0$ we expect that the system is in a localized phase, with all bosons in the lowest lying, localized single-particle eigenstate. Note that due to the finite size of the calculation, D_s does not vanish even at $U = 0$. Nevertheless, the bounds D_s^* and D_s^o do capture the large suppression of D_s at small U , while the mean kinetic energy is clearly unable to do so. For intermediate U we find nonmonotonic U -dependence in D_s [14]. From a mathematical point of view, there is no guarantee that because D_s is a nonmonotonic function of some parameter, say U , an upper bound on D_s should show similar U -dependence. It is therefore interesting that this feature is captured by all the bounds. At larger values of U , D_s^* and D_s^o are closer to the KE in value, than to D_s , but all three track the overall trend of D_s fairly well.

In Fig. 6 we keep the interaction U fixed and study D_s and the bounds as a function of disorder strength V_{dis} . We find that D_s decreases monotonically with disorder. This trend is captured by all three bounds, however, we clearly see that D_s^* does increasingly better than the other bounds in the large disorder regime.

VI. Remarks:

In this Section we collect together some remarks which are meant to clarify different points which we feel are important. We also consider a model where the bound D_s^* captures a transition unlike in the examples presented earlier.

Charge Stiffness versus Superfluid Stiffness

A bound similar to the mean kinetic energy bound (10) has been discussed in Ref. [16] in connection with the charge stiffness, which is the coefficient of $\delta(\omega)$ in the optical conductivity of a perfect conductor. We emphasize that although the linear response formalism leads to essentially identical bounds for both the charge stiffness and the superfluid stiffness D_s , the variational wavefunction construction of Section IV and the associated bounds are valid only for D_s . Recall that the charge stiffness is defined in terms of the energy of the adiabatically generated ground state as the twist is introduced [6]. The variational ansatz that is considered here is by construction a trial ground state of the system at finite twist and is not an adiabatic continuation of the untwisted ground state. We therefore emphasize that unless there is a gap which makes the charge and superfluid stiffness equal [6], the above variational construction does not give us a bound on the charge stiffness.

Kinetic Energy : Exact versus Approximate Estimates

We should note that our bounds are expressed in terms of the local kinetic energies evaluated in the *exact* ground state which is in general not known. Nevertheless, one can derive useful qualitative information simply from the form of the bounds. In order to get quantitative estimates of the bounds and of D_s one needs to resort to numerical methods like QMC. However, the bounds which involve local correlations, are much less affected by finite size errors.

If a trial ground state wave function is used, instead of the exact one, to evaluate the local kinetic energies, then the expressions derived above do *not* lead to rigorous upper bounds. Such approximations could, nevertheless, lead to useful estimates.

Quantum Percolation Model

We now describe an example which highlights a qualitative difference between the bounds D_s^* and D_s^o and where D_s^* in fact captures a phase transition unlike earlier examples of both clean and disordered systems. Consider a “quantum bond percolation model” of bosons on a lattice with hopping disorder such that the hopping matrix element between two neighbouring sites is either t , with probability $(1-p)$, or zero with probability p . We assume that the twist is applied along a certain direction and that we have fixed boundary conditions in the perpendicular directions.

As the probability p of having a “broken link” increases, the superfluid stiffness reduces until it vanishes at some $p = p_{loc}$ via a (quantum) *localization transition*. We do not expect either D_s^* or D_s^o to show a signature of this transition. The bound D_s^* would go to zero when there is *any* set of broken links that can break up the lattice into two disconnected parts across the twist direction. Thus we expect D_s^* to vanish at $p = p_c$ corresponding to the *classical bond percolation transition* and $p_c > p_{loc}$. In order for D_s^o to vanish, the lattice needs to be disconnected along a (hyper)plane *perpendicular to the twist direction*. Since the hopping matrix elements are chosen randomly, realizations with such a set of broken links will be of measure zero. Thus D_s^o will not capture this percolation transition.

Bounds on T_c in 2D:

In two dimensions an upper bound on the superfluid density allows us to put an upper bound on the superfluid to normal transition temperature T_c in a clean system. For this we use the relation between the jump in superfluid density at the Kosterlitz-Thouless (KT) transition and the KT transition temperature [17] $D_s(T_c^-) = 2T_c$ (with $k_B = 1$). Thus, $D_s(T_c^-) \leq D_s^*(T_c) \leq D_s^*(T = 0)$ which gives us the following bound on T_c :

$$T_c \leq D_s^*(T_c)/2 \leq D_s^*(T = 0)/2. \quad (26)$$

Note, however, that in general a lower superfluid density at zero temperature does not necessarily imply a lower T_c . A counterexample is the case of s-wave BCS superconductors with weak disorder: Anderson’s theorem tells us that in this case T_c and other thermodynamic properties are unaffected but one would expect D_s to be suppressed by the disorder.

VII. Conclusions

In this paper we have obtained several upper bounds on the superfluid stiffness at zero temperature as well as finite temperatures. These have been obtained using the Kubo linear response formalism as well as variational estimates. These bounds give qualitative insight into the dependence of D_s on various parameters.

For clean systems, the average kinetic energy $\langle K_1 \rangle$ gives a good upper bound on D_s/π and provides insight into the difference between lattice and translationally invariant (continuum) models. The bound captures the qualitative trend of the superfluid stiffness D_s to decrease with increasing repulsive interaction U . For incommensurate filling, the bound compares well with D_s at all values of the interaction. At commensurate filling, the bound is good at small values of U but fails to capture the superfluid-Mott insulator transition at large U .

For disordered systems we obtain two improved variational bounds D_s^* and D_s^o ($D_s^* \leq D_s^o \leq \pi \langle K_1 \rangle$) by allowing larger phase twists on links with lower local kinetic energy. We quantitatively compare the bounds with QMC results and find that they capture non-trivial parameter dependence of D_s , including its nonmonotonic variation in some cases.

Appendix

Path Integral Quantum Monte Carlo

In this Appendix we briefly describe the path integral QMC method used to calculate the local kinetic energies and the superfluid stiffness D_s presented in the paper. For more details see Refs. [18,19]. The notation in this appendix differs from that in the rest of the paper since here we work in first quantized representation. The position vector of the n^{th} boson, $n = 1 \dots N_b$, at imaginary time τ , where $0 \leq \tau \leq \beta$, is denoted by $\mathbf{r}_n(\tau)$. The diagonal density matrix for bosons in the canonical ensemble is given by

$$\rho(R, R; \beta) = \frac{1}{N_b!} \sum_{\mathcal{P}} \langle R | \exp(-\beta H) | \mathcal{P}[R] \rangle \quad (27)$$

which describes the amplitude for the N_b -particle system starting in a configuration $R = \{\mathbf{r}_1, \mathbf{r}_2, \dots, \mathbf{r}_{N_b}\}$ at time $\tau = 0$ to be in configuration $\mathcal{P}[R]$, where \mathcal{P} is a permutation of R , at time $\tau = \beta = 1/T$. The partition function is given by $Z = \sum_R \rho(R, R; \beta)$. Each particle describes a path or a world-line in the \mathbf{r} - τ space, and the evaluation of the partition function amounts to summing over all possible paths which is most efficiently done by QMC techniques.

The first step in evaluating the density matrix is to break the total time β into small steps $\delta\tau = \beta/N_\tau$. Upon inserting complete sets of states we get

$$\rho(R, R; \beta) = \frac{1}{N_b!} \sum_{\mathcal{P}} \sum_{R_1} \sum_{R_2} \dots \sum_{R_{(N_\tau-1)}} \rho(R, R_1; \delta\tau) \rho(R_1, R_2; \delta\tau) \dots \rho(R_{(N_\tau-1)}, \mathcal{P}[R]; \delta\tau) \quad (28)$$

A particular configuration of the particles on all the time slices, is denoted by

$$\mathcal{S} = [\mathcal{P}; R, R_1, R_2, \dots, R_{(N_\tau-1)}, R_{N_\tau}] \quad (29)$$

and looks like a collection of strings. Our aim is to sample the probability function

$$\text{Prob}[\mathcal{S}] = \rho(R, R_1; \delta\tau) \rho(R_1, R_2; \delta\tau) \dots \rho(R_{(N_\tau-1)}, \mathcal{P}[R]; \delta\tau) \quad (30)$$

We use the Metropolis importance sampling method to generate a sequence of M string configurations $\mathcal{S}_1, \mathcal{S}_2, \dots, \mathcal{S}_M$ such that in the limit $M \rightarrow \infty$ the probability of finding a particular configuration \mathcal{S}_μ in this sequence is proportional to $\text{Prob}[\mathcal{S}_\mu]$. The actual implementation of the Monte Carlo method, including importance sampling, and the bisection method for efficient exploration of phase space, is described in Ref [19].

Calculation of the Local Kinetic Energy

For simplicity, first consider an operator $O = \sum_i f(\hat{n}_i)$ which is diagonal in the position basis, like the interaction energy in the second term of eqn.(13) (similar considerations apply to the disorder energy in eqn.(25)). Then

$$\langle O \rangle \equiv \frac{\text{Tr} O e^{-\beta H}}{\text{Tr} e^{-\beta H}} = \frac{1}{M} \sum_{\mu=1}^M \frac{1}{N_\tau} \sum_{\tau=1}^{N_\tau} \sum_i f(n_i^\mu(\tau)) \quad (31)$$

where $n_i^\mu(\tau)$ is the number of bosons at site i on time slice τ in the string configuration \mathcal{S}_μ .

Next, consider the local kinetic energy operator given in eqn.(3). Recall that in the Monte Carlo procedure, the density matrix in an elemental time $\delta\tau$ is approximated by

$$\rho(R_\tau, R_{\tau+1}) = \prod_{n=1}^{N_b} \rho_1(\mathbf{r}_n^\mu(\tau), \mathbf{r}_n^\mu(\tau+1)) \times \exp \left[-(\delta\tau/2) \sum_j [\mathcal{U}_i^\mu(\tau) + \mathcal{U}_i^\mu(\tau+1)] \right] \quad (32)$$

where ρ_1 is the single particle density matrix corresponding to the kinetic energy and disorder potential operators and $\mathcal{U}^\mu(n_i(\tau)) = (U/2)n_i^\mu(\tau)(n_i^\mu(\tau) - 1)$ arises from the interaction between the bosons.

To evaluate the kinetic energy, pick a string configuration \mathcal{S}_μ with the n^{th} boson at $\mathbf{r}_n^\mu(\tau)$ on time slice τ and imagine moving that boson to one of its four neighboring sites $\mathbf{r}'_n^\mu(\tau)$ on the same time slice generating a new configuration. For clarity, we suppress the μ index labelling a configuration in the following equations. The change in potential energy is given by $\mathcal{U}_{new} - \mathcal{U}_{old}$.

$$U_{old} = \mathcal{U}[n(\mathbf{r}_n(\tau))] + \mathcal{U}[n(\mathbf{r}'_n(\tau))] \quad (33)$$

and

$$U_{new} = \mathcal{U}[n(\mathbf{r}_n(\tau)) - 1] + \mathcal{U}[n(\mathbf{r}'_n(\tau)) + 1] \quad (34)$$

There will also be a change in the single particle density matrix.

Thus the local kinetic energy for a given string configuration \mathcal{S}_μ is

$$K(\mathbf{r}_n(\tau), \mathbf{r}'_n(\tau)) = \frac{\rho_1(\mathbf{r}'_n(\tau), \mathbf{r}_n(\tau + 1))}{\rho_1(\mathbf{r}_n(\tau), \mathbf{r}_n(\tau + 1))} \exp[-U_{new} + U_{old}] \quad (35)$$

which is then averaged over all the configurations selected by the Monte Carlo procedure.

Calculation of Superfluid Stiffness D_s

The current along the α^{th} direction is given by

$$j_\alpha(\tau) = \sum_{n=1}^{N_b} [r_{n\alpha}(\tau + \delta\tau) - r_{n\alpha}(\tau)]/\delta\tau \quad (36)$$

where $r_{n\alpha}(\tau)$ is the α^{th} component of $\mathbf{r}_n(\tau)$ ($\alpha = 1 \dots d$). The winding number W_α which counts the number of times the path of a particle winds around a box with periodic boundary conditions is given by [20]

$$W_\alpha = \frac{1}{N_\tau} \sum_{\tau=1}^{N_\tau} j_\alpha(\tau) \quad (37)$$

and the superfluid stiffness is given by

$$\frac{D_s}{\pi} = L^{2-d} \sum_\alpha \langle W_\alpha^2 \rangle \quad (38)$$

In the case of Fig.4, we calculate the winding number, the stiffness and the bounds all along the x -direction only as indicated in the figure inset. For all other figures, we calculate the total D_s given in eqn.(38).

[1] P. Nozieres and D. Pines, “ The Theory of Quantum Liquids ” (Vol.II), (Addison Wesley, 1990), Sec 4.2, p.55.

[2] M.P.A. Fisher, P.B. Weichmann, G. Grinstein and D.S. Fisher, *Phys. Rev.* **B40**, 546 (1989).

[3] T.V. Ramakrishnan, *Physica Scripta* , **T27**, 24 (1989).

[4] A. J. Leggett, *Phys. Rev. Lett.* **25**, 1543 (1970).

[5] G. Baym, in “Mathematical Methods in Solid State theory and Superfluidity ”, edited by R.C. Clark and G.H. Derrick, (Oliver and Boyd, Edinburgh, 1969).

[6] D.J. Scalapino, S.R. White and S.C. Zhang, *Phys. Rev.* **B47**, 7995 (1993).

[7] For a system with uniform hopping, but a dispersion $\epsilon(\mathbf{k})$ more general than nearest neighbor hopping, the diamagnetic piece $\langle K_1 \rangle$ gets replaced by $\sum_{\mathbf{k}} n(\mathbf{k}) \text{Tr} [m^{-1}(\mathbf{k})]$, where $m_{\alpha,\beta}^{-1}(\mathbf{k}) \equiv \partial^2 \epsilon(\mathbf{k}) / \partial \mathbf{k}_\alpha \partial \mathbf{k}_\beta$.

[8] N. Byers and C.N. Yang, *Phys. Rev. Lett.* **7**, 46 (1961).

[9] M.E. Fisher, M.N. Barber and D. Jasnow, *Phys. Rev.* **A8**, 1111 (1973).

[10] As an example, consider a 2D Fermi system described by the negative U Hubbard model for which QMC data is available; see, e.g., N. Trivedi, R.T. Scalettar and M. Randeria, *Phys. Rev. B* **54**, R3756 (1996). From Fig. 1 of this reference we find that (for zero disorder) $D_s/\pi \simeq 0.56$ and $\langle K_1 \rangle \simeq 0.68$ in units where $t = 1$. This difference points to the importance of fluctuations beyond mean field theory (MFT), which would have given $D_s/\pi = \langle K_1 \rangle$ at $T = 0$. The finite $T = 0.1$ by itself cannot account for this difference within MFT since the BCS gap $\Delta(0) \sim 1 \gg T$.

[11] W. Krauth and N. Trivedi, *Europhys. Lett.* **14**, 627 (1991).

[12] G.V. Chester in “Helium Liquids: Proceedings of the 15th Scottish Universities Summer School in Physics”, edited by G.M. Armitage and I. E. Farquhar, (Academic, New York, 1975).

[13] The inequality $D_s^* < D_s^0$ continues to hold in the continuum case as well, with obvious changes like $K_1(\mathbf{r})$ being replaced by the density $n(\mathbf{r})$. The bound D_s^* should be useful for continuum systems with disorder and also for systems, such as the one considered in Ref. [4], in which translational invariance is spontaneously broken.

[14] W. Krauth, N. Trivedi, and D. Ceperley, *Phys. Rev. Lett.* **67**, 2307 (1991).

[15] G. G. Batrouni, R. T. Scalettar, and G. T. Zimanyi, *Phys. Rev. Lett.*, **65**, 1765 (1990); R. T. Scalettar, G. G. Batrouni, and G. T. Zimanyi, *Phys. Rev. Lett.*, **66**, 3144 (1991).

[16] A.J. Millis and S.N. Coppersmith, *Phys. Rev.* **B42**, 10807 (1990).

[17] D.R. Nelson and J.M. Kosterlitz, *Phys. Rev. Lett.* ,**39**, 1201 (1977).

[18] D.M. Ceperley, *Rev. Mod. Phys.* **67**, 279 (1995).

[19] *Quantum Monte Carlo Simulations for Disordered Boson Systems*, N. Trivedi, in “Computer Simulations in Condensed Matter Physics V”, edited by D. P. Landau, K. K. Mon, and H. B. Schuttler, (Springer Verlag, Heidelberg, Berlin, 1993).

[20] D.M. Ceperley and E.L. Pollock, *Phys. Rev.* **B39**, 2084 (1989).

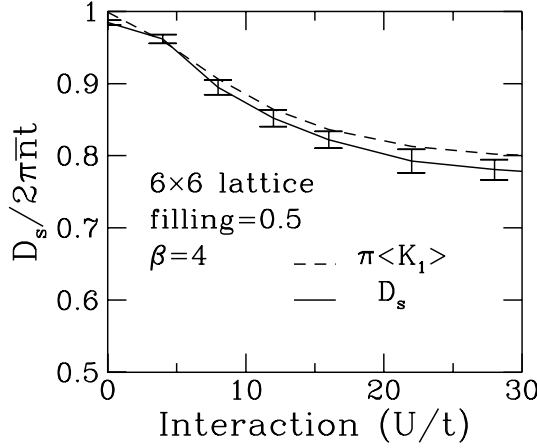


FIG. 1. The superfluid stiffness D_s and the KE bound $\pi\langle K_1 \rangle$ obtained from path integral QMC for the Boson Hubbard model in eqn. (13) at an incommensurate filling $\bar{n} = 0.5$ for parameter values shown in the figure. The QMC data here (and in other figures) was averaged over 10^8 runs to sufficiently reduce error bars in order to allow comparison with the bounds. The normalization here and in the remaining figures is chosen to make the normalized stiffness unity for a clean non-interacting system at $T = 0$ independent of the filling factor.

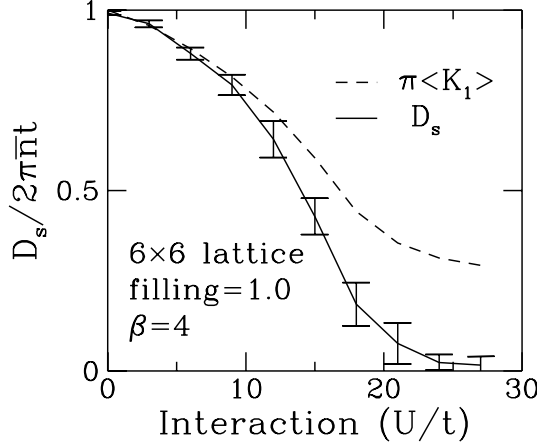


FIG. 2. Superfluid stiffness D_s and KE bound $\pi\langle K_1 \rangle$ for the Boson Hubbard model (13) plotted for commensurate filling \bar{n} and parameter values indicated in the figure. In the thermodynamic limit, D_s would vanish for $U > U_c$ (where $U_c/t \sim 20$) signalling the superfluid to Mott insulator transition while on a finite system it remains non-zero even beyond that value and is zero (within error bars) only at large U . The bound however is clearly non-zero even at large U and can be shown from perturbation theory to go as t^2/U for $t \gg U$. The bound *does not* capture the Mott transition.

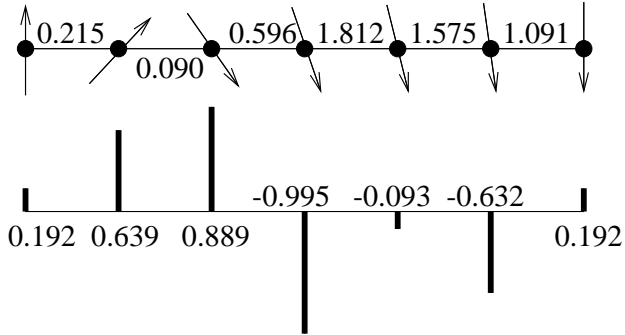


FIG. 3. The phase $\theta(\mathbf{r})$ calculated at each site (shown as arrows) indicating how the applied phase twist $\Phi = \pi$ is accommodated along the lattice in a one-dimensional case for a particular realization of disorder for the dirty boson problem of eqn. (25). The absolute value of the kinetic energy is indicated along the links and the disorder potential is shown in the lower part of the figure (both in units of t .) The “bad bonds” (the first two links with smaller kinetic energy) allow for a greater phase twist across them as shown. The data was obtained by exact diagonalization for a system of 4 bosons on a 6-site chain.

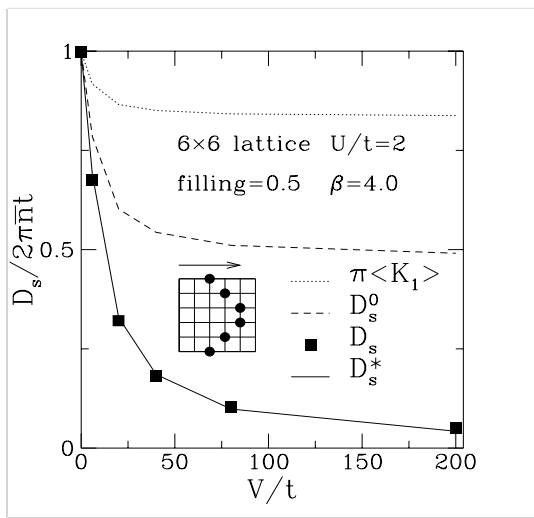


FIG. 4. Superfluid stiffness plotted for a 6×6 system at incommensurate filling in which the sites indicated in the inset are kept at a potential V with the rest kept at a potential of zero. The phase twist is applied along the direction shown by the arrow in the inset and the bounds and the stiffness D_s are obtained only along that direction. The error bars on D_s are of the size of the data point and hence not indicated. The difference between the various bounds is evident. Notice that the bound D_s^* is better than the other bounds by about an order of magnitude.

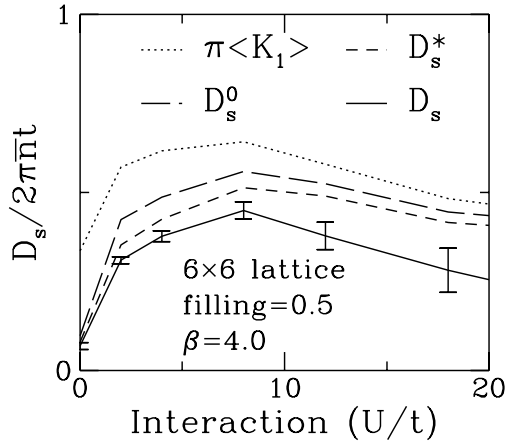


FIG. 5. Superfluid stiffness plotted as a function of interaction U for the dirty boson problem in eqn. (25) at incommensurate filling for $V_{dis}/t = 10$ and other parameter values indicated in the figure. The bounds capture the non-monotonic behavior of D_s obtained from QMC as a function of U . The bound D_s^* is clearly better than the KE bound when compared with D_s . At large U , the kinetic energies on various links are more uniform and the bounds are closer to each other.

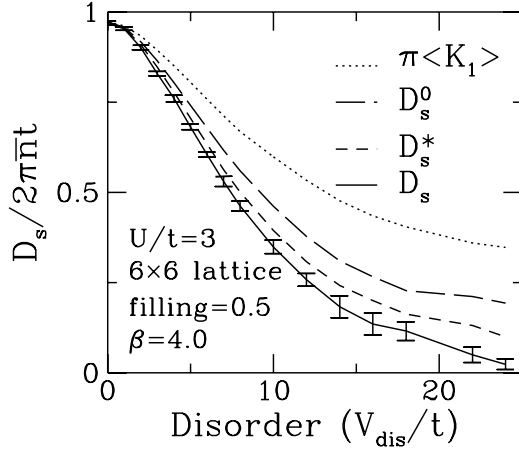


FIG. 6. Stiffness plotted as a function of disorder, V_{dis} , for the dirty boson problem in eqn. (25) at incommensurate filling for parameter values indicated in the figure. The bound D_s^* gets progressively better than the other two bounds in the disorder dominated regime. This is precisely the regime where the local kinetic energies are very inhomogeneous.